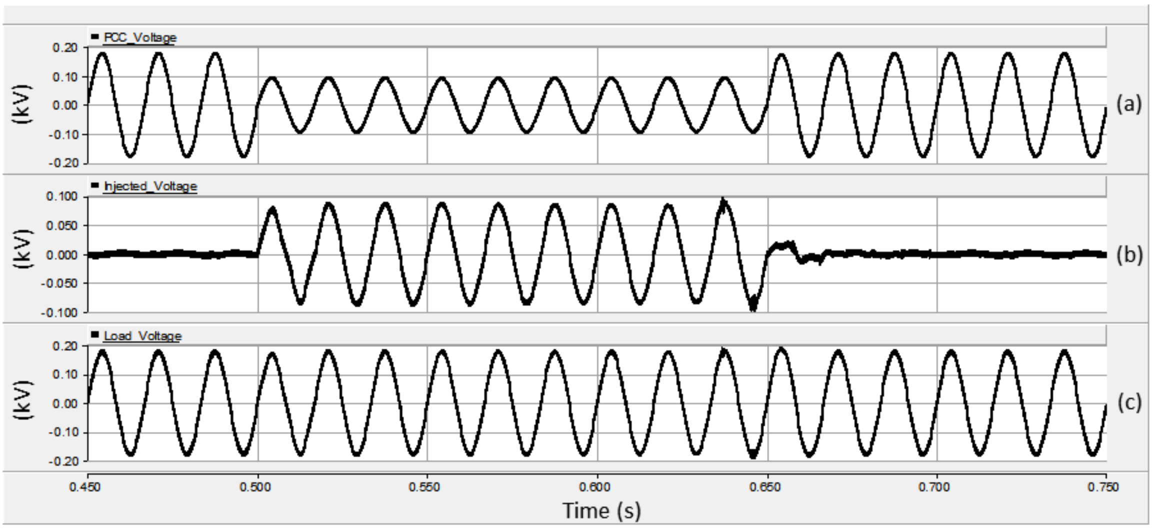

Fig. 12. Result showing voltage sag. (a) PCC voltage. (b) Compensation voltage. (c) Load voltage.

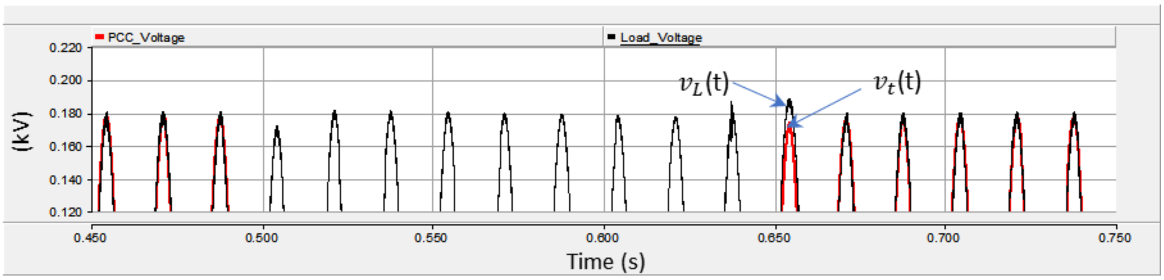

Fig. 13. Detail Load voltage and Pcc voltage.

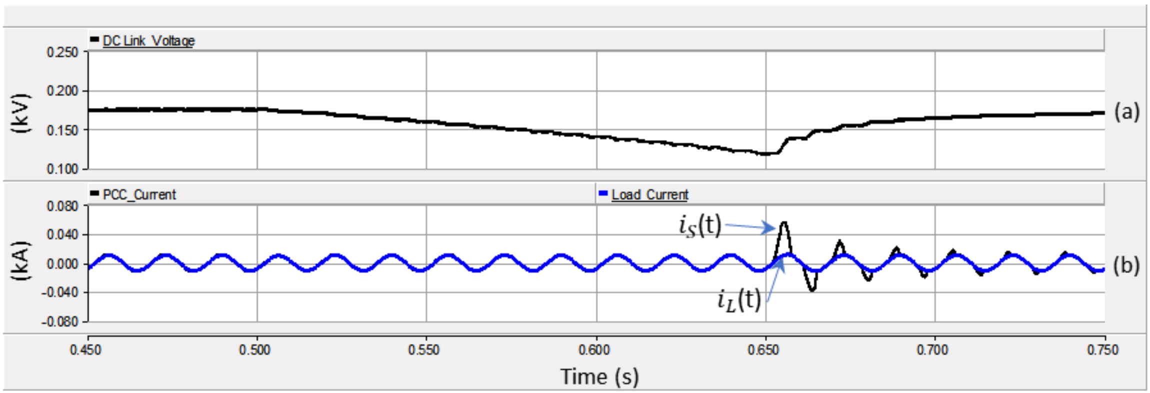

Fig. 14. Result showing voltage sag. (a) DC-Link voltage. (b) Supply and load Currents.

Case 2. Grid voltage condition under voltage swell.

The voltage will increase to 117.39% of its normal value, for duration of 0.15 sec, between t = 0.5 sec to t = 0.65 sec. Figure 15 shows the simulation results of supply voltage, compensating voltage, compensated load voltage during voltage swell. PCC voltage peak value is 178 V, load voltage peak value 177.1 and load voltage ripple is 6.9 V peak to peak. The lowest value during the voltage swell is 173.4 V and the highest value relative to the voltage swell transitory period was 179.2 V. These variations are within the established limits of ± 5V.

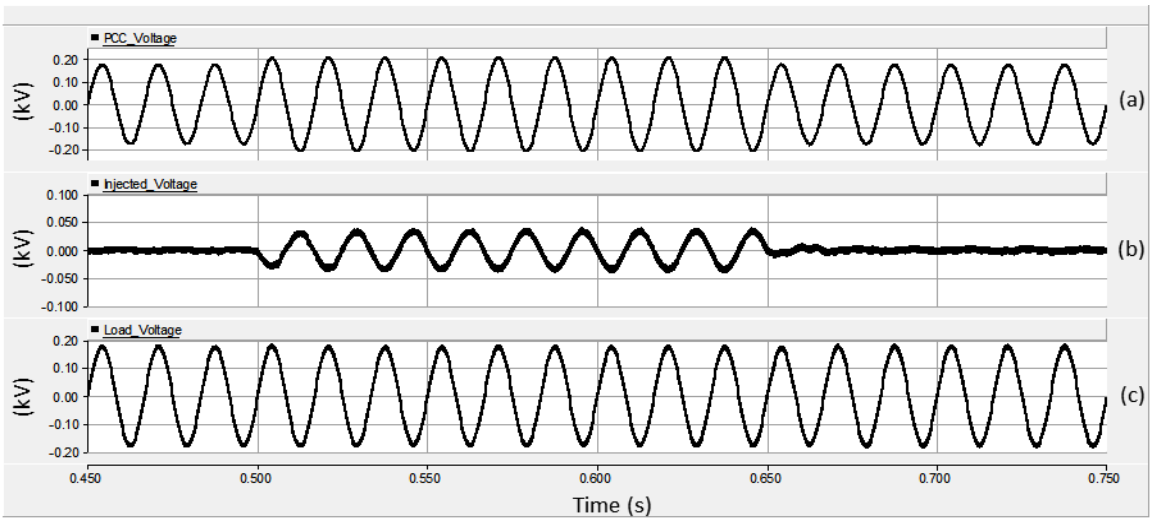

Fig. 15. Result showing voltage swell. (a) PCC voltage. (b) Compensation voltage. (c) Load voltage.

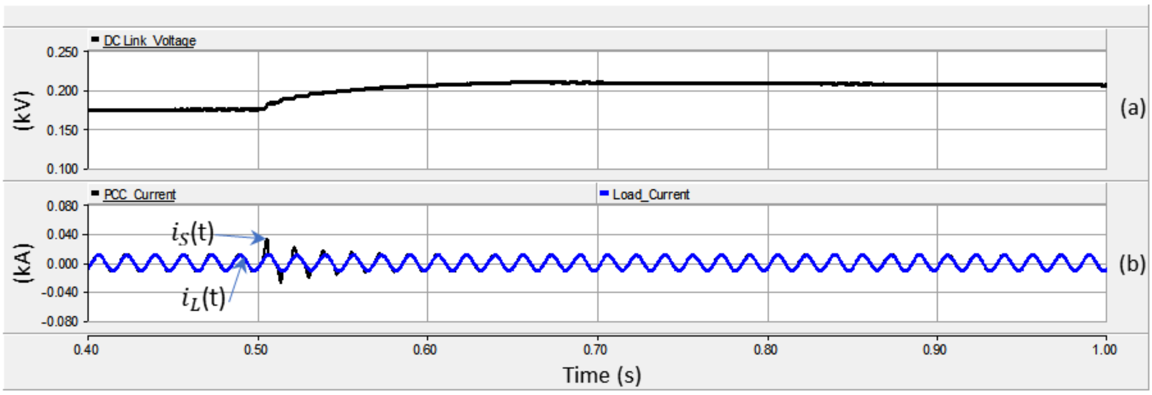

Fig. 16. Result showing voltage swell. (a) DC-Link voltage. (b) Supply and load Currents.

Figure 16 depicts DC link voltage, supply and load currents. In this case the dynamic behavior is different, and the DC link voltage has a slower transient response. However, the source current has a distinct dynamic and is associated with the DC link voltage rise and has reached a lower peak value.

The dynamic behavior of the voltage at the DC link showed in Figure 14(a) can be more accurately verified in a duration of 5 sec. as shown in Figure 17. The effective steady state was settled after 4.1 sec. In this case also, the use of a controlled rectifier would represent a better dynamic performance. But this would be another aspect to be discussed in terms of cost versus benefit.

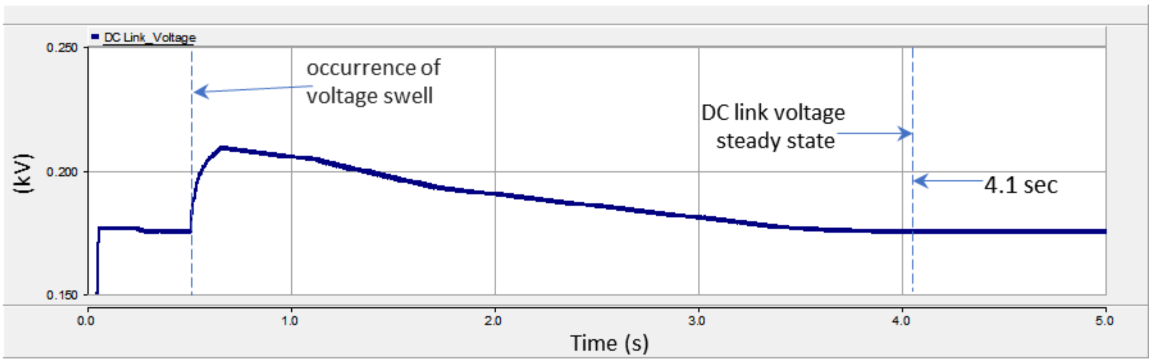

Fig. 17. DC-Link voltage

Case 3. Grid voltage condition under voltage harmonics.

The sinusoidal source voltage will be distorted to a THD% = 24.79% (44.31V), for duration of 0.2sec, between t = 0.5 sec to t = 0.7 sec. The harmonics adopted were $V_3 = 21.97\,V$, $V_5 = 32.35\,V$, $V_7 = 20.79\,V$. Figure 18 shows the simulation results of supply voltage, compensating voltage, compensated load voltage during voltage harmonics disturbance.

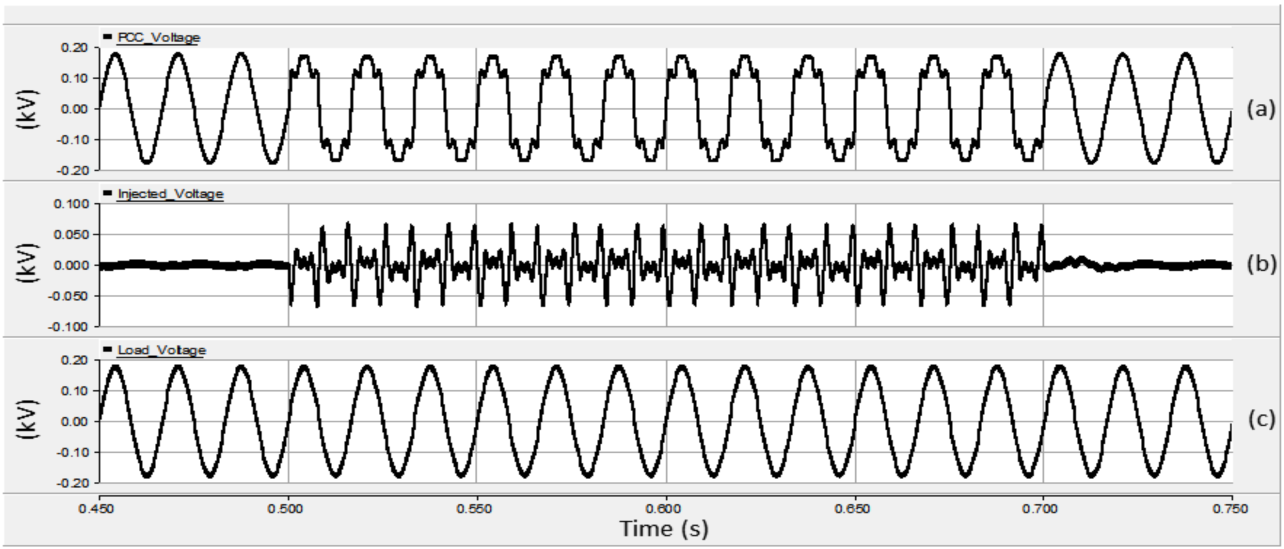

Fig. 18. Result showing voltage harmonics. (a) PCC voltage. (b) Compensation voltage. (c) Load voltage.

In this case, as expected, a small variation in the DC link voltage was observed in Figure 19(a).

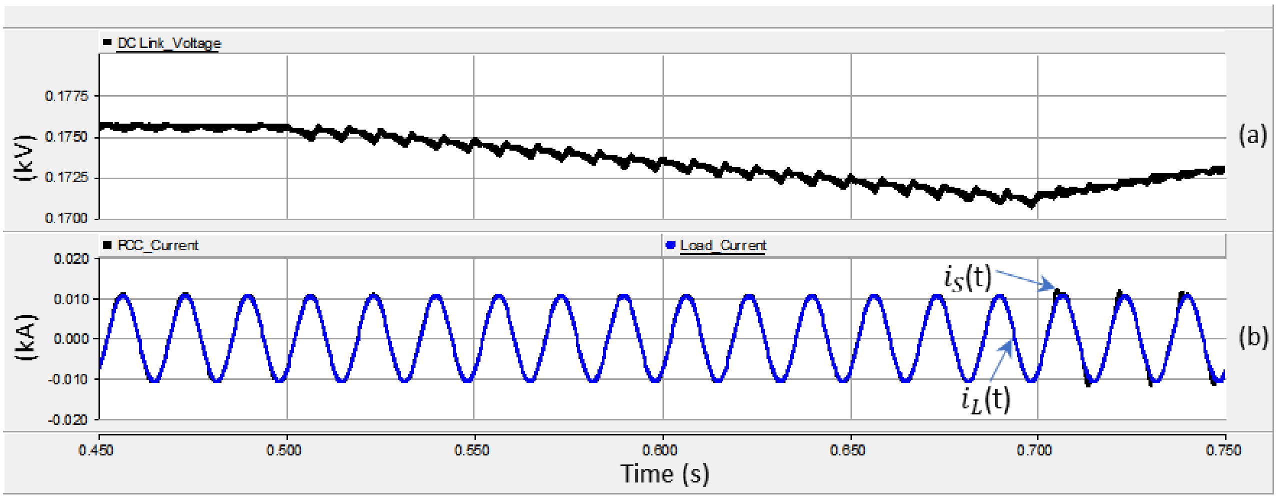

Fig. 19. Result showing voltage harmonics. (a) DC-Link voltage. (b) Supply and load Currents.

The behavior of the current at the source shows that only a small amount of energy was needed to recover the value of the DC link as can be verified in Figure 19(b). The harmonics distortions values of the PCC and load voltages obtained are depicted in Figure 20.

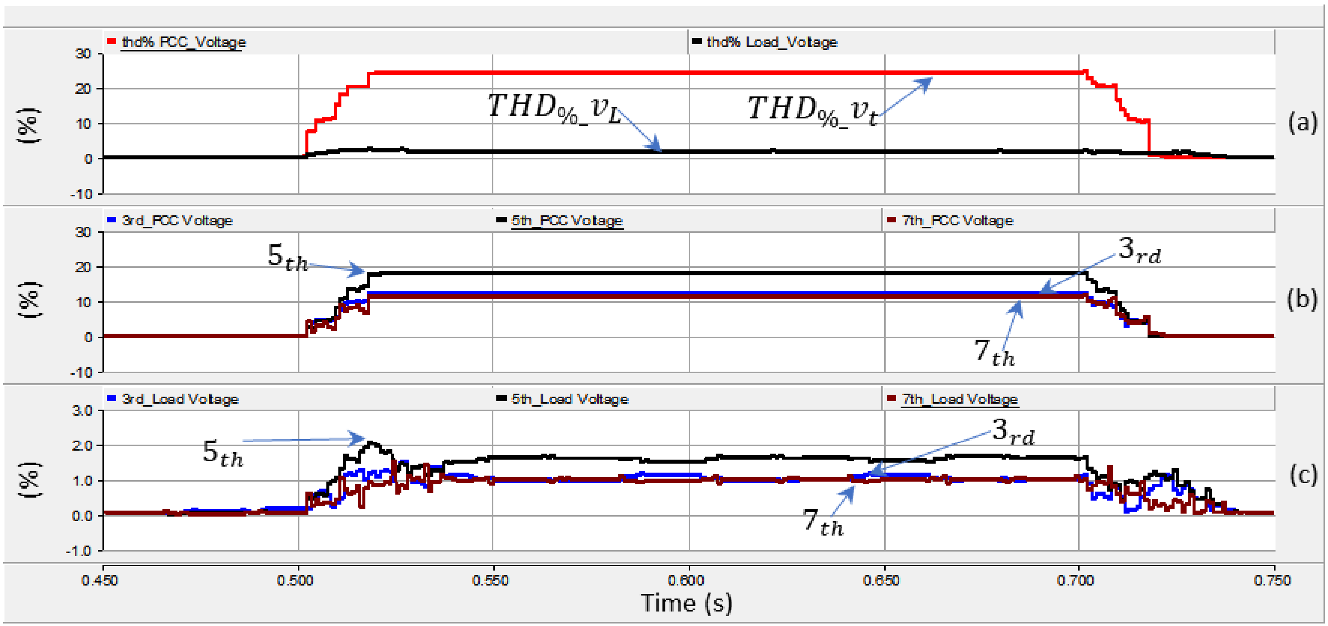

Fig. 20. Result showing voltage harmonics. (a) Total harmonic distortion. (b) PCC voltage harmonics. (c) Load voltage Harmonics.

Table 3 resumes the behavior between the periods of 0.2sec in which the voltage harmonics were injected in the grid voltage.

Table 3. THD and harmonic values during the period which the PCC voltage were distorted.

Voltage harmonics distortion	**PCC voltage**	**Load voltage**
THD(%)	24.81	2.25
3^{th}(%)	12.31	1.02
5^{th}(%)	18.14	1.69
7^{th}(%)	11.78	1.04

Case 4. Grid voltage condition under voltage harmonics and sag.

In this case, two simultaneous disturbance are implemented for DVR compensation. First, the sinusoidal source voltage will be distorted to a THD% = 24.79% (44.31V) from 0.3 sec and maintaining distortion during simulation analysis. The harmonics adopted were $V_3 = 21.97\,V$, $V_5 = 32.35\,V$, $V_7 = 20.79\,V$. Second, the supply voltage will decrease to 52.17 % of its normal value, for duration of 0.15 sec, between t = 0.5 sec to t = 0.65 sec.

Figure 21 shows the performance of the proposed controller by compensating first voltage harmonics and during 0.15sec compensating voltage harmonics and voltage sag. The DC link voltage drops during voltage sag and recovers relatively slowly from the energy from the uncontrolled rectifier as shown in Figure 22(a). Figure 22(b) illustrate the behavior of the supply current and can be verified the transient after voltage sag ends in 0.65 sec. This transient which initially represented a high current value is associated with the energy replacement for the DC link capacitor through the uncontrolled rectifier.

The harmonics distortions values of the PCC and load voltages obtained before, during and after sag voltage period are depicted in Figure 23. Table 4 shows the harmonic distortions values after compensation of the voltage disturbances before and during voltage period.

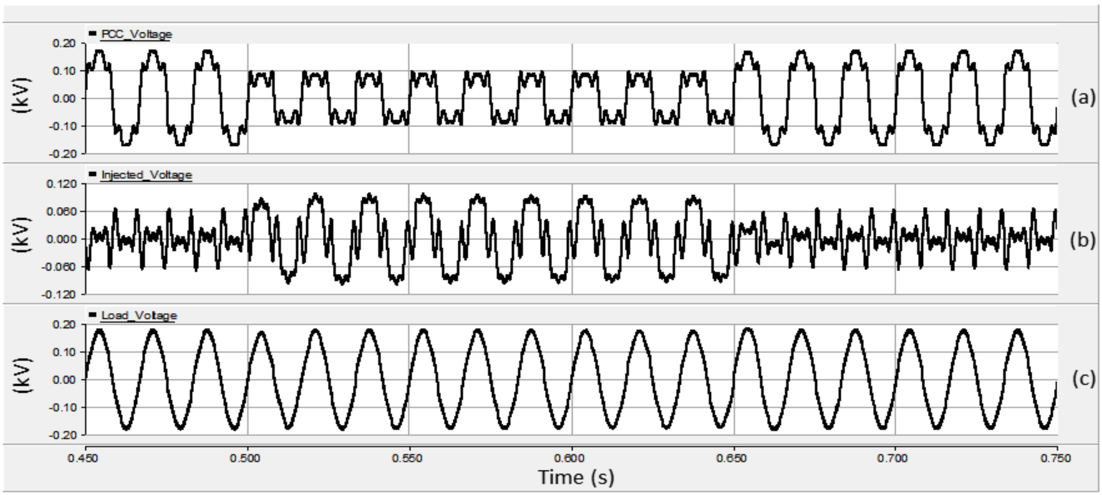

Fig. 21. Result showing voltage harmonics and sag. (a) PCC voltage. (b) Compensation voltage. (c) Load voltage.

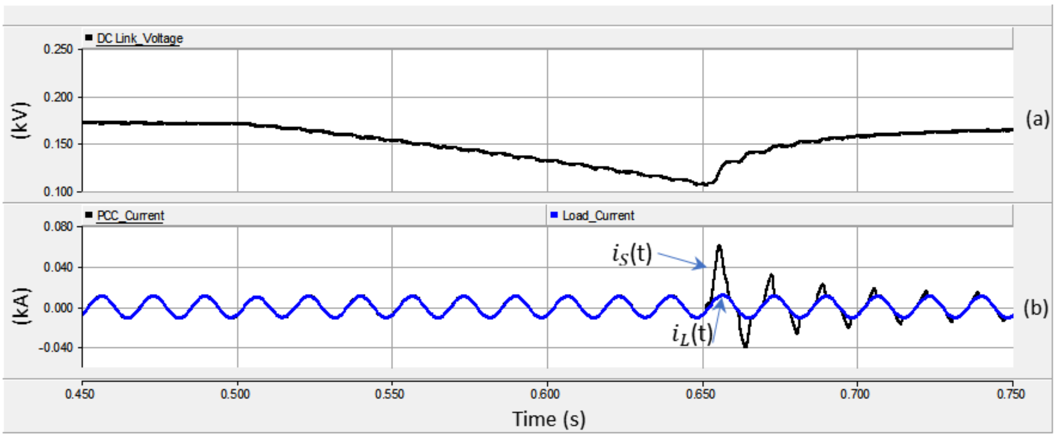

Fig. 22. Result showing voltage harmonics and sag. (a) DC-Link voltage. (b) Supply and load Currents.

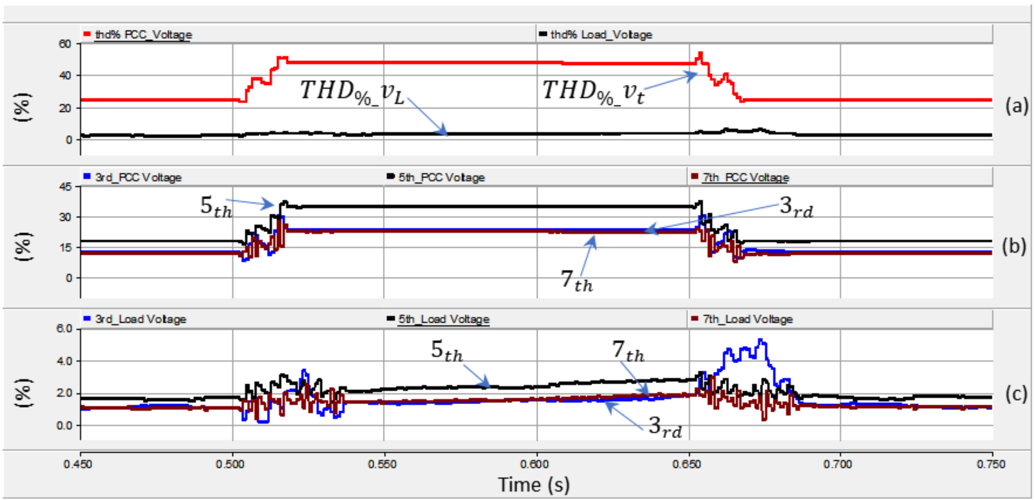

Fig. 23. Result showing voltage harmonics and sag. (a) Total harmonic distortion. (b) PCC voltage harmonics. (c) Load voltage Harmonics

Table 4. THD and harmonic values after voltage compensation.

Voltage Harmonics Distortion	PCC voltage	PCC voltage (during Sag period)	Load voltage DVR connected	Load voltage DVR connected (during SAG period)
THD(%)	24.82	47.79	2.26	3.64
3^{th}(%)	12.33	23.70	1.09	1.61
5^{th}(%)	18.13	34.92	1.64	2.73
7^{th}(%)	11.77	22.43	1.06	1.80

CONCLUSIONS:

This work, a novel algorithm for extraction reference voltage for extraction of voltage harmonics and detection of sag/swell of single-phase DVR is shown. The voltage reference algorithm is based on a detector that extract fundamental component and instantaneous magnitude of measured PCC voltage. The voltage reference signal is used in indirect voltage control with a SPWM switching technique. The proposed control strategy has been analyzed, presented and validated in a single-phase DVR with power supply upstream of the series transformer using PSCAD/EMTDC. The single-phase DVR performance is investigated under steady-state and transient conditions and found satisfactory, confirming that the control strategy complies with its goals, allowing the DVR to compensate main voltage harmonics and voltage sag/swell. These simulations indicate that control strategy has a very good accuracy under steady-state conditions and a fast dynamic response in transient situations. It should be noted that the voltage values measured in the load with the operation of the DVR were within the limits reported in section III, proving the effectiveness of the proposed. In this DVR topology, the DC bus voltage is unregulated and voltage sag/swell must be compensating within operational limits.

REFERENCES

[1] IEEE Std 519-1992, "IEEE Recommended Practices and Requirements for Harmonic Control in Electric Power Systems", Institute of Electrical and Electronics Engineers, Inc. 1993.

[2] ANSI C84.1-2011 ELECTRIC POWER SYSTEMS AND EQUIPMENT - VOLTAGE RANGES (American National Standard for Electric Power Systems and Equipment – Voltage Ratings (60 Hertz).

[3] IEC 61000-4-30. Electromagnetic Compatibility (EMC) -Part 4-30: Testing and measurement techniques -Power quality measurement methods.

[4] IEEE Std. 1159-1995. IEEE recommended practice for monitoring electric power quality. Technical report, The Institute of Electrical and Electronics Engineers, Inc., 1995.

[5] Prafull A. Desale, Vishvadeep J. Dhawale, and Ranjeet M. Bandgar. Brief Review Paper on the Custom Power Devices for Power Quality Improvement, International Journal of Electronic and Electrical Engineering. ISSN 0974-2174 Volume 7, Number 7 (2014), pp. 723-733.

[6] Nielsen J. G. and Blaabjerg F. A detailed comparison of system topologies for dynamic voltage restorers. IEEE Trans. Ind. Appl. 41(5): 1272–1280, 2005.

[7] Y. W. Li, D. M. Vilathgamuwa, F. Blaabjerg, and P. C. Loh, "A robust control scheme for medium – voltage level DVR implementation," IEEE Trans. Ind. Electron., vol. 54, no. 4, pp. 2249–2261, Aug. 2007.

[8] Li, B.H.; Choi, S.S.; Vilathgamuwa, D.M., "Transformerless dynamic voltage restorer," Generation, Transmission and Distribution, IEE Proceedings- , vol.149, no.3, pp.263-273, May 2002.

[9] Y, Xiao G, Lei B, Wu X and Zhu S 2014 A transformerless active voltage quality regulator with the parasitic boost circuit. IEEE Trans. Power Electron. 29(4): 1746–1756

[10] B. Bae, J. Lee, J. Jeong, and B. Han., Line-Interactive Single-Phase Dynamic Voltage Restorer With Novel Sag Detection Algorithm, IEEE TRANSACTIONS ON POWER DELIVERY, VOL. 25, NO. 4, OCTOBER 2010, pp. 2702-2709

[11] Y.W. Li, D.M. Vilathgamuwa, F. Blaabjerg, and P.C. Loh, "A robust control scheme for medium-voltage-level DVR implementation," IEEE Trans. Ind. Electron., Vol. 54, No. 4, pp. 2249-2261, Aug. 2007.

[12] U. WAQAS, M. A. M. RADZI, N. MARIUN DYNAMIC VOLTAGE RESTORER FOR EFFICIENT DETECTION AND COMPENSATION OF VOLTAGE SAG USING ANN BASED LMS AS A NEW CONTROL STRATEGY, Journal of Engineering Science and Technology Special Issue on Applied Engineering and Sciences, October (2014), pp. 21 – 29 © School of Engineering, Taylor's University

[13] Series compensation to mitigate harmonics and voltage sags/swells in distributed generation based on symmetrical components estimation, 2011 IEEE International Symposium on Industrial Electronics – ISIE, 2011

[14] Amit Kumar, Deepak Kumar, Abhay Yadav, MITIGATION OF POWER QUALITY PROBLEMS AND HARMONICS COMPENSATION USING CAPACITOR-SUPPORTED DYNAMIC VOLTAGE RESTORER (DVR), Journal of Electrical Engineering, pp. 1-12

[15] Mustafa INCI, Mehmet BUYUK, Adnan TAN, Kamil Cagatay BAYINDIR, Mehmet TUMAY, Multipurpose

Compensation Scheme for Voltage Sag/Swell and Selective Harmonics Elimination in Distribution Systems, 2018 ADVANCES IN ELECTRICAL AND ELECTRONIC ENGINEERING, POWER ENGINEERING AND ELECTRICAL ENGINEERING VOLUME: 16, NUMBER: , 2018, MARCH.

[16] S. S. Choi, B. H. Li, D. M. Vilathgamuwa, “Design and Analysis of the Inverter-Side Filter Used in the Dynamic Voltage Restorer”, IEEE Transactions on Power Delivery, Vol.17, No.3, pp. 857-864, July 2002.

[17] S. S. Choi, B. H. Li , D. M. Vilathgamuwa, “Design Considerations on the Line-Side Filter Used in the Dynamic Voltage Restorer”, IEE Proc.-Gener. Distrib, Vol.148, No.1, pp. 1-7, January 2001.

[18] A. D. Sousa ; J. A. Moor Neto ; J. C. Ferreira ; M. S. dos Reis ; L. Peres, Fast and robust fundamental component estimation algorithm for a single phase system. 2017 Brazilian Power Electronics Conference (COBEP), Brazil., pp-1-6

[19] Ayhan Özdemir, Irfan Yazici, Cabir Vural; Fast and robust software-based digital phase-locked loop for power electronics applications, IET Gener. Transm. Distrib., 2013, Vol. 7, Iss. 12, pp. 1435–1441

[20] M. P. Kazmierkowski and L. Malesani, “Current control techniques for three-phase voltage-source PWM converters: a survey,” Industrial Electronics, IEEE Transactions on, vol. 45, no. 5, pp. 691–703, 1998.

[21] M. Ramasamy, S. Thangavel Photovoltaic based dynamic voltage restorer with power saver capability using PI controller Int J Electr Power Energy Syst, 36 (2012), pp. 51-59.

[22] Samet Biricik, and Hasan Komurcugil, Optimized Sliding Mode Control to Maximize Existence Region for Single-Phase Dynamic Voltage Restorers, IEEE TRANSACTIONS ON INDUSTRIAL INFORMATICS, VOL. 12, NO. 4, AUGUST 2016, pp. 1486-1497

[23] Alireza Javadi, Abdelhamid Hamadi, Lyne Woodward, and Kamal Al-Haddad, Experimental Investigation on a Hybrid Series Active Power Compensator to Improve Power Quality of Typical Households, IEEE TRANSACTIONS ON INDUSTRIAL ELECTRONICS, VOL. 63, NO. 8, AUGUST 2016, pp. 4849-4859.

[24] Dhiraj N. Katole, M. B. Daigavane, S. P. Gawande, Prema Daigavane G.H.R.C.E., Modified instantaneous p-q theory for single phase DVR for mitigation of voltage sag in case of nonlinear load, 2016 International Conference on Electrical Power and Energy Systems (ICEPES) Maulana Azad National Institute of Technology, Bhopal, India. Dec 14-16, 2016, pp. 163-168